Journal of Aerospace Technology and Management
ISSN: 1984-9648
secretary@jatm.com.br
Instituto de Aeronáutica e Espaço
Brasil

Carvalho Mazzeu, Maria Alice; Komorek Faria, Lohana; de Moura Cardoso, Andreza; Medeiros Gama, Adriana; Ribeiro Baldan, Maurício; Sarmento Gonçalves, Emerson
Structural and Morphological Characteristics of Polyaniline Synthesized in Pilot Scale
Journal of Aerospace Technology and Management, vol. 9, núm. 1, enero-marzo, 2017, pp. 39-47
Instituto de Aeronáutica e Espaço
São Paulo, Brasil

doi: 10.5028/jatm.v9i1.726

Structural and Morphological Characteristics of Polyaniline Synthesized in Pilot Scale

Maria Alice Carvalho Mazzeu[1,2], Lohana Komorek Faria[3,4], Andreza de Moura Cardoso[3], Adriana Medeiros Gama[3], Maurício Ribeiro Baldan[5], Emerson Sarmento Gonçalves[1,3]

ABSTRACT: Polyanilines have many applications in Aerospace, especially in their doped form. Studies on their synthesis in a pilot scale can contribute to obtain products with desirable characteristics for such applications. The present study reports the chemical oxidative synthesis of polyaniline in pilot scale and different reaction times in order to determine if there are variations in the polyaniline structure, morphology and conductivity due to these synthesis conditions. It is very common to analyze these data for polymers obtained through bench scale. However, several parameters change the properties of final material in major scales, such as thermal, mechanic and diffusive variables. Therefore, the reaction time is the only variable into the 9 syntheses carried out, and polyaniline is obtained in a doped form, being dedoped with ammonium hydroxide and redoped with dodecylbenzenesulphonic acid. The doped and redoped samples were characterized by their molecular structure, thermal behavior, crystallinity and morphology. The electrical conductivity of redoped samples was determined. Some differences in the structure and morphology of doped and dedoped forms, identifying the doping structures, were reported. This paper aims to present the relationship between changes on structure and morphology of doped and undoped polyaniline obtained by the mentioned experiments. Furthermore, some addicts on conductivity are carried out. It was possible to contribute in order to obtain a more conductive polyaniline in pilot scale.

KEYWORDS: Polyaniline, Crystallinity, Morphology, Raman spectroscopy, Electrical conductivity.

INTRODUCTION

Since the observation of the remarkably high electrical conductivity of a halogen-treated polyacetylene, a number of other conjugated polymers have shown transition from an insulating to a highly-conductive state, such as polyaniline (PAni), poly (phenylenevinylene), polypyrrole, and polythiophene. Because of their unique electrical properties covering the whole insulator-semiconductor-metal range, unusual conducting mechanism as well as controllable chemical and electrochemical properties, conducting polymers show not only great potential in a range of applications, but also great contribution to the fundamental materials science research (Luo *et al.* 2011).

Among conducting polymers, PAni has received wide-spread attention because of its outstanding properties including simple and reversible doping-dedoping chemistry, stable electrical conduction mechanisms, high environmental stability and ease of synthesis (MacDiarmid 2001; Fratoddi *et al.* 2015).

Nevertheless, PAni exhibits poor physical and mechanical properties and is insoluble in common solvents (Panah *et al.* 2012). To improve solubility and induce fusibility of the stiff chain of this polymer, a doping procedure with functionalized protonic acids such dodecylbenzenesulfonic acid (DBSA) can be used (Jaymand 2013). The DBSA enhances the solubility and the stability of the PAni, and the complex salt exhibits a good conductivity. However, the emulsion needs a high DBSA/PAni molar ratio because some molecules of DBSAs act as a dopant

1.Departamento de Ciência e Tecnologia Aeroespacial – Instituto Tecnológico de Aeronáutica – Programa de Pós-Graduação em Ciência e Tecnologias Espaciais – São José dos Campos/SP – Brazil. **2.**Departamento de Ciência e Tecnologia Aeroespacial – Instituto de Fomento e Coordenação Industrial – Divisão de Certificação de Sistema de Gestão – São José dos Campos/SP – Brazil. **3.**Departamento de Ciência e Tecnologia Aeroespacial – Instituto de Aeronáutica e Espaço – Divisão de Materiais – São José dos Campos/SP – Brazil. **4.**Universidade do Vale do Paraíba – Faculdade de Engenharia, Arquitetura e Urbanismo – São José dos Campos/SP – Brazil. **5.**Instituto Nacional de Pesquisas Espaciais – Laboratório Associado de Sensores – São José dos Campos/SP – Brazil.

Author for correspondence: Maria Alice Carvalho Mazzeu | Departamento de Ciência e Tecnologia Aeroespacial – Instituto de Fomento e Coordenação Industrial – Divisão de Certificação de Sistema de Gestão | Praça Marechal Eduardo Gomes, 50 – Vila das Acácias | CEP: 12.228-900 – São José dos Campos/SP – Brazil | Email: aie.mzz@hotmail.com

Received: Jun. 16, 2016 | **Accepted:** Aug. 20, 2016

of PAni, and the others act as a surfactant to keep the stability of the reactive medium (Kohut-Svelko *et al.* 2005).

PAni has potential utilization in a large number of applications: rechargeable batteries, sensors, electronic devices, light-emitting diodes, conducting paints and glues, gas-separation membranes, coatings etc. (Ibrahim 2013). Moreover, many studies have been conducted regarding application of PAni in the aerospace sector, and some of these applications are cited next.

The lifetime and efficiency of electronic devices and electrical equipment can be increased through effective electromagnetic interference (EMI) shielding. Conducting polymers such as doped polyaniline or polypyrrole are promising materials to replace or supplement typical metals for EMI shielding applications. Conducting polymers have merits such as lightweight, physical flexibility, and a tunable shielding response (Joo and Lee 2000).

The stealth technology makes use of geometrical means and material engineering in order to develop low reflection and high absorption structures. The most suitable way of reducing the reflection is by covering the aircraft with Radar Absorbing Materials (RAM) as of paint or polymeric sheet (Franchitto *et al.* 2007). Conducting polymers have been applied as RAM due to the possibility of variation in their conductivity with the frequency of the incident radiation (Faez *et al.* 2000).

Aircrafts routinely operate in atmospheric environments that, over time, may affect their structural integrity. Despite using appropriate materials and process for protection, recurrent exposure to chlorides, pollution, temperature gradients, and moisture provide the necessary electrochemical conditions for the development and profusion of corrosion in aircraft structures (Rinaldi *et al.* 2012). There are several new technologies now under consideration for aluminum alloys protection including conductive polymers as primers without Cr-based metal pre-treatments (Bierwagen 2001). For magnesium and its alloys, the conducting polyaniline-blended organic coatings have been found to protect the pinholes due to the passivation ability of the conductive polymer (Sathiyanarayanan *et al.* 2008).

Since commercial airliners are struck by lightning quite often during their operation, there is a need to elaborate new materials for lightning strike protection combining high conductivities with lightweight. Conducting polymers are thought to be one of the most promising compounds that can be used for this application. From a variety of commercially available conducting polymers, PAni fits the criteria of the best chemical stability, appropriate conductivity, and density (Krukiewicz and Katunin 2016).

These applications require PAni at industrial scale, and the optimization of manufacturing processes is essential for this purpose. Since pilot scale influences the hydrodynamics of polymerizations system (Roichman *et al.* 1999), this kind of experiment is important for evaluating amendments in the process.

In this study, each synthesis was performed on a pilot scale, with variation of reaction time for every synthesis, keeping the other parameters unchanged. The PAni salt first obtained was dedoped, and the PAni in a base form, non-conductive (PAni-B) was redoped with DBSA, when PAni in a salt form, conductive (PAni-DBSA) was achieved. The effects of synthesis conditions on the structural and morphological characteristics of PAni-B and PAni-DBSA are investigated by Raman spectroscopy, thermogravimetric analysis (TGA), X-ray diffractometry (XRD), and scanning electron microscopy (SEM). Electrical conductivity was determined for redoped samples.

METHODOLOGY

Synthesis of PAni-B in different reaction times: 9 syntheses of polyaniline powder were obtained by the usual chemical oxidative polymerization of aniline with ammonium peroxydisulfate (APS). For each synthesis, aniline (1.0 M) and APS (1.9 M) solutions have been prepared separately, in aqueous solution containing 1.0 M hydrochloric acid and 1.0 M sodium chloride; the synthesis was performed in a 5-L glass reactor with glass rods and Teflon naval type propellers, for agitation. The reactor temperature was maintained at -5 ± 1°C.

Aniline solution was added to the reactor under constant stirring, and then APS solution was added dropwise. The reactions started with the oxidant addition and stopped 10; 20; 35; 50; 65; 80; 95; 110 and 170 min after the beginning. Fifty minutes were necessary for the complete addition of APS so, in the first 3 syntheses, it was not completely added yet. The polyaniline salts obtained were filtered and washed with approximately 10 L of distilled water until the washing liquid was colorless and the pH was around 6.

Dedoping process: PAni-B was prepared by dedoping of the powder in a 1.0-M ammonium hydroxide solution, being

held under agitation by 12 h. The material was filtered again, washed, and the power (dark brown color) was dried in a conventional oven at 60 °C until constant weight. Figure 1 represents the chemical structure of PAni-B, according to Galiani *et al.* (2007).

Redoping process: PAni-B (5 g) was added to an aqueous solution containing 9 g of DBSA and left under constant stirring for 24 h at room temperature. The doped PAni-DBSA was washed with distilled water and ethyl alcohol, filtered, and the green powder was drying under vacuum at 60 °C until constant weight. The chemical structure of PAni-DBSA is represented in Fig. 2 (Galiani *et al.* 2007).

To confirm the chemical structures of PAni-B and PAni-DBSA, including doping, it was used a Raman spectrometer Labram HR Evolution, with Argon ion laser at 514 nm. A thermogravimetric analyzer model 7HT (PerkinElmer®) was used to study moisture content and thermal behavior of the polymers. The crystallinity study was performed by an X-ray diffractometer Panalytical, model XPert PRO, with a rotating anode X-ray generator working at $5° \leq 2q \leq 90°$, with Cu Kα monochromatic radiation of 0.154 nm; to study the surface morphology, it was employed a Zeiss Leo 440 SEM. AC electrical conductivity measurements were carried out by dielectric impedance spectroscopy (DIS), with a 2-terminal probe arrangement, by using a potentiostat-galvanostat AUTOLAB PGSTAT302 with impedance module.

Samples were used in powdered form, without dilution for all techniques, except for conductivity measurements, when the powder was compacted up to 3 MPa to obtain the pellets.

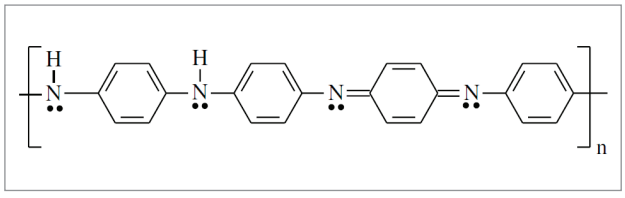

Figure 1. Chemical structure of PAni-B.

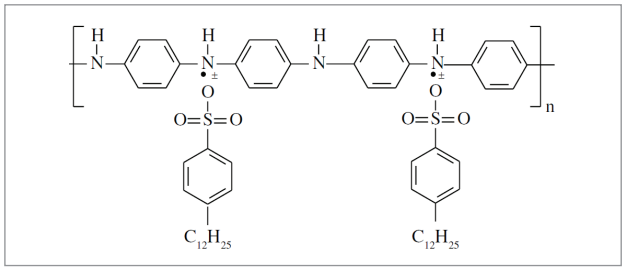

Figure 2. Chemical structure of PAni-DBSA.

RESULTS AND DISCUSSION

RAMAN SPECTROSCOPY

Raman spectroscopy has demonstrated to be a useful analytical tool to investigate conducting polymers (Engert *et al.* 1994). Raman spectra of PAni-B and PAni-DBSA, at 110 min reaction time, are presented in Fig. 3.

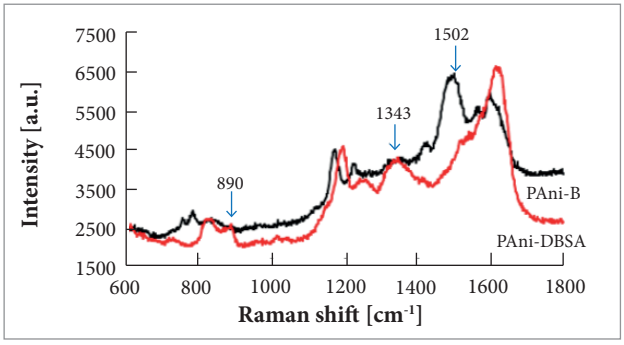

Figure 3. Raman spectra of PAni-B and PAni-DBSA (lO = 514 nm).

PAni-B spectra presented characteristic bands at 1170 (C-H bending); 1206 (C-N stretching); 1502 (C=N stretching); 1560 (N-H bending) and 1598 cm^{-1} (C=C stretching) (Mažeikienė *et al.* 2007; Cirić-Marjanović *et al.* 2008; Moravková *et al.* 2012). PAni-DBSA spectra, in turn, presented characteristic bands at 1190 (C-H bending); 1,260 (C-N stretching); 1,343 ($C-N^+$ stretching); 1,530 (C-C stretching); and 1620 cm^{-1} (C-H stretching) (Nobrega *et al.* 2012; Ibrahim 2013; Shakoor and Rizvi 2010).

The conductive nature of PAni-DBSA can be associated to the band located at 890 cm^{-1} (arrow in Fig. 3), assigned to deformation C-N of secondary amine next to aromatic ring in the polaronic form $C-N^+-C$, and to the band at 1343 cm^{-1} (arrow in Fig. 3) that is assigned to vibration of a delocalized polaron structure (Belaabed *et al.* 2010). The band at 1502 cm^{-1} (arrow in Fig. 3), which is assigned to C=N, is very intense for PAni-B but significantly decreases to PAni-DBSA, due to the association between PAni and DBSA. Figures 1 and 2 illustrate what happens with the band assigned to C=N, where one can observe changes in the chemical structure due to the doping process.

THERMOGRAVIMETRIC ANALYSIS

The knowledge of PAni's thermal stability is important for its use in many practical applications. The thermal degradation of PAni is shown by thermogravimetry (Gul *et al.* 2013).

TGA results for PAni-B, PAni-DBSA, and DBSA are shown in Fig. 4, and the differential thermogravimetry curves (DTG), calculated from TGA, are shown in Fig. 5.

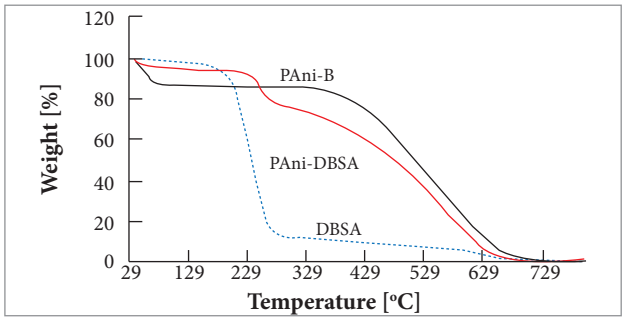

Figure 4. Thermogravimetric curves of PAni-B, PAni-DBSA, and pure DBSA.

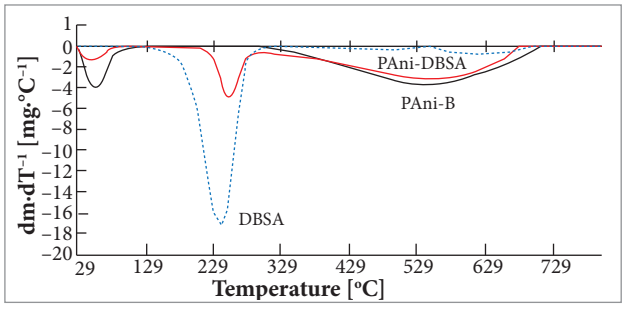

Figure 5. DTG curves of PAni-B, PAni-DBSA, and pure DBSA.

The temperature ranges mentioned next refer to measurements carried out at room temperature and atmospheric air.

PAni-B presents 2 stages of weight loss. The first weight loss occurs in the range of ~ 30 to 90 °C and is related to the loss of physically absorbed water plus moisture evaporation and, perhaps, outgassing of unknown small molecules (Zeng andKo 1998; Nithyaprakash *et al.* 2014). The second weight loss, starting at ~ 330 °C and finishing at ~ 700 °C, is attributed to complex and irreversible processes of decomposition of the polymeric chain (Nobrega *et al.* 2012).

PAni-DBSA also presents a first weight loss in the range of ~ 30 to 80 °C and a second one at ~ 130 to 290 °C, attributed to breakdown of the interaction between the PAni chain and the DBSA dopant ($NH^+....SO_3^-$), with decomposition of DBSA. The decomposition temperature is higher than that of pure DBSA. A third weight loss that starts at ~ 300 °C and is complete at ~ 680 °C indicates a structural decomposition of the PAni backbone (Babazadeh 2009). Weight losses obtained from thermogravimetric curves of PAni-B and PAni-DBSA are shown in Table 1.

Table 1. Weight losses results from PAni-DBSA and PAni-B.

Event	Weight losses (%)	
	PAni-DBSA	PAni-B
Water + moisture evaporation	3.0	7.8
DBSA decomposition	12.9	------
PAni decomposition	70.3	59.8
Residual weight	13.8	32.4

Thermal behavior change is observed when comparing PAni associated with DBSA molecules. The degradation temperature is higher than that of pure DBSA, and PAni decomposition begins before than PAni-B, probably due to PAni-DBSA interaction. This interaction affects the weight losses too, and higher values are obtained for PAni decomposition, probably due the chain is more vulnerable when associated with DBSA. The results of thermal degradation have shown that PAni-DBSA could be used for applications where high temperature is necessary.

ELECTRICAL CONDUCTIVITY

The 2-probe and 4-probe techniques are commonly used to characterize almost all semiconductor products available in the world today. These techniques have paved the way in discovering semiconductor materials (Ashraf 2014; Barsoukov and MacDonald 2005).

Two-probe is the simplest method for measuring resistivity and it is useful when the sample has large resistance. It is used mainly for the measurement of high-impedance materials where the impedance of cables is not significant (Barsoukov *et al.* 2005).

Considering that conductivity is the inverse of resistivity, in this study the conductivity was obtained by utilizing the 2-probe method to measure the electrical resistivity of PAni-DBSA, using Eq. 1 (Abed *et al.* 2014):

$$R = \rho\, L/A \qquad (1)$$

where: R is the electrical resistance; ρ is the electrical resistivity; L is the length of the material in the direction of the current; A is the cross-sectional area.

The conductivity s (S/cm) was calculated according to Eq. 2:

$$\sigma = 1/\rho \qquad (2)$$

The electrical conductivity for some reaction times is presented in Table 2.

Table 2. Electrical conductivity of PAni-DBSA.

Reaction time (min)	50	80	95	110	170
Electrical conductivity ($S \cdot cm^{-1}$)	1.8×10^{-5}	4.6×10^{-6}	4.0×10^{-7}	4.0×10^{-4}	8.1×10^{-4}
Error ($S \cdot cm^{-1}$)	4.22×10^{-7}	2.08×10^{-6}	6.54×10^{-8}	5.14×10^{-5}	3.61×10^{-5}

The sample preparation may interfere with the results since the sample is pressed. However, these results confirm that conductive structures are present at PAni-DBSA, as Raman spectroscopy has shown.

The obtained PAni-DBSA is a semiconductor, and a 170-min reaction time shows the highest electrical conductivity result.

For applications, PAni-DBSA is normally used as a blend with others materials which serve as a support. Such materials may be rubber, paint, silicone or other polymers and they may influence electrical conductivity too.

X-RAY DIFFRACTOMETRY ANALYSIS

XRD is used for the determination of the crystallinity degree of polymeric compounds (Araujo *et al.* 2013). Crystalline orientation of conducting polymer is very interesting, because a more highly-ordered system could display a metallic property such as conductive state (Vivekanandan *et al.* 2011), but the crystallinity of polyaniline and the intensity of peaks depend on the synthesis conditions (Pouget *et al.* 1991; Laska and Widlarz 2005). Polyanilines are semi-crystalline in nature and a 2-phase system. The phase in which the polymer chains are parallel and ordered in close packed array is the crystallites region, while the phase where the chains are not ordered and do not have parallel alignment is the amorphous region (Bhadra and Khastgir 2008). The faster grown of the polymer results in disorder orientation of polymer chains and amorphous polymer structure (Kumar *et al.* 2013).

Figure 6 shows XRD patterns of PAni-B and PAni-DBSA for a reaction time of 110 min. The diffraction patterns of PAni-DBSA agree with Soares *et al.* (2006), in relation to redoped method of preparation, and the diffraction patterns of PAni-B agree with Zilberman *et al.* (1997). The crystalline phase can be identified in both XRD spectra; however, PAni-DBSA shows 2 peaks at 2θ = 20 and 25° while PAni-B shows 4 peaks at 2θ = 10; 15; 20 and 25°, which is an indicative of more ordered structures than PAni-DBSA.

Besides the preparation methods, other factors may contribute to differences in crystallinity of PAni-B and PAni-DBSA, such as variation in inter-chain hydrogen bonding and electrostatic interaction at these times, polymer morphology, as well as speed of polymer formation.

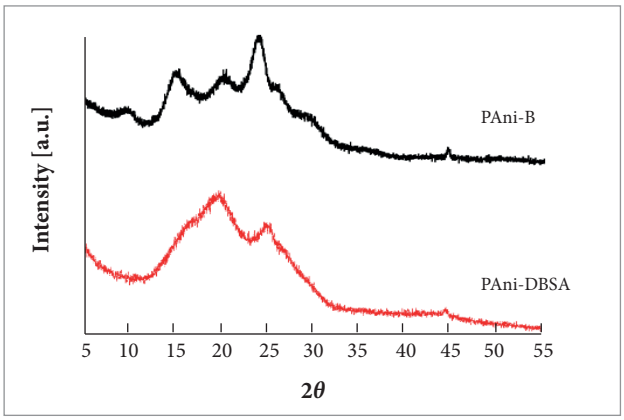

Figure 6. XRD pattern of PAni-B and PAni-DBSA.

The proportion between amorphous phase contributions in overall structure (R) of PAni-B and PAni-DBSA, in each reaction time, was calculated using the ratio between minimum and heights of peaks, as described in Saravanan *et al.* (2006) and Manjunath *et al.* (1973).

For PAni-DBSA pattern, R was calculated using Eq. 3, with minimum and heights of the peaks at 2θ = 20 and 25°.

$$R = 2m_1/h_1 + h_2 \quad (3)$$

where: m_1 represents the heights of minima between 2 peaks; h_1 and h_2 are the heights of these peaks from the base.

For PAni-B spectrum, R was calculated using Eq. 4, with minimum and height of the sharp peaks at 2θ = 15; 20; and 25°.

$$R = m_1 + 2m_2/h_1 + h_2 + h_3 \quad (4)$$

where: m_1 and m_2 are the heights of minima between 2 peaks; h_1, h_2, and h_3 are the heights of peaks from the base.

Crystallinity indexes were given by 1-R, and the results for PAni-B in each reaction time are shown in Fig. 7.

Crystallinity index for PAni-B showed variation against the reaction time, with some specific higher values like 50

and 170 min. Since each reaction is unique, the changes in the crystallinity index seem to be more related to speed of formation of the polymer than to reaction time.

Crystallinity index results for PAni-DBSA in each reaction time are shown in Fig. 8 and present very slight variation. The main factors that can influence these results are the method of preparation (dedoping-redoping) and the fact that DBSA is a bulky dopant. The previously synthetized material (PAni-B) appears to have little influence on the crystallinity of the redoped PAni (PAni-DBSA).

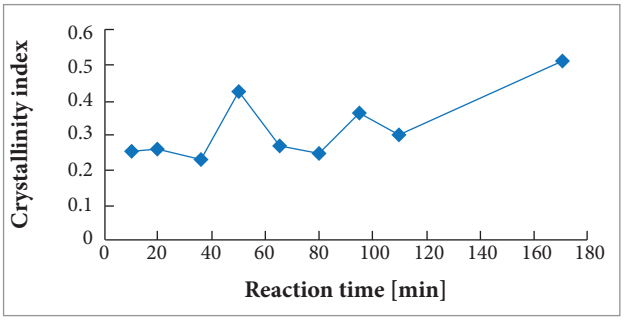

Figure 7. Crystallinity index variation with reaction time for PAni-B.

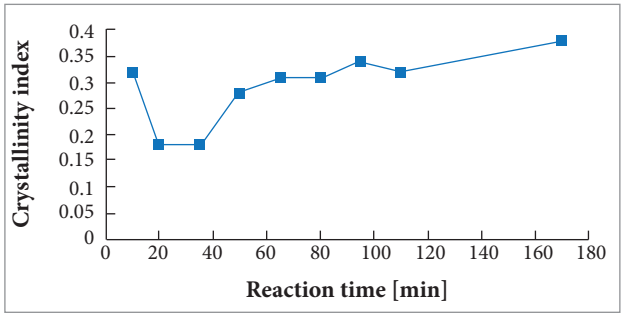

Figure 8. Crystallinity index variation with reaction time for PAni-DBSA.

SCANNING ELECTRON MICROSCOPY

The formation of PAni morphology is determined by the synthesis conditions (Abdolahi *et al.* 2012). The granular morphology of PAni powders is most common in PAni prepared by precipitation polymerization when using strong oxidants and high aniline concentrations under strongly-acidic conditions, at pH < 2.5. Globular structure has often been used as a synonym of the granular type (Stejskal *et al.* 2010).

Polyaniline prepared in this way is highly aggregated, and rapid sedimentation from solution is generally observed. However, careful examination reveals that a small quantity of nanofibers also appear in the product. Apparently, these nanofibers are formed without any extra structural directing agents, suggesting that nanofibers may be a natural morphology of polyaniline (Huang and Kaner 2006).

Most relevant morphological characteristics of PAni-B and PAni-DBSA are shown in Fig. 9. It is rather hard to distinguish the individual particles or grains from the images because the particles are aggregated. Therefore, it is difficult to identify the size and shape of the grains.

The structures more discernible at PAni-B (Fig. 9a, obtained at 110 min) that appear at any reaction time are tiny coral reefs closely covered with globules (or granules). In our synthesis condition, it is expected that the formed spheres or fibers tend to agglomerate, forming micro-particles. At reaction time of 50 and 170 min (Fig. 9b, arrow, obtained at 170 min), it is possible to identify several structures that appear to be fiber by linking agglomerates structures. These structures seem to be more related with agglomeration phenomena during the synthesis than with time of reaction, and it could cause deviations in analysis by XRD.

PAni-DBSA showed agglomerates of globular structures, similarly to PAni-B, but with forms that are more spherical and with some flatter multilayer structure (Fig. 9c, obtained at 110 min). PAni-DBSA also showed some shapeless areas, ascribed to the high concentration of dopant (Fig. 9d, arrow, obtained at 170 min).

After PAni-B is redoped and PAni-DBSA is obtained, the reaction time seems to have no influence on morphology.

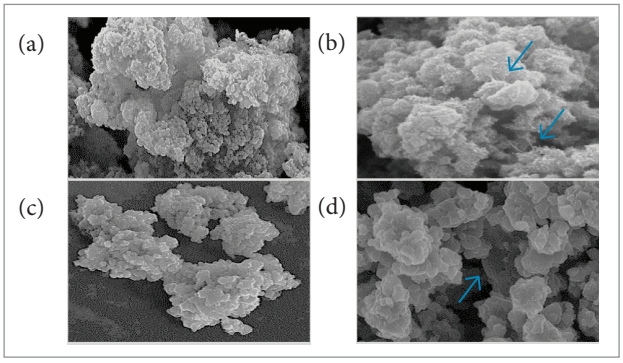

Figure 9. Most relevant morphological characteristics. (a, b) PAni-B; (c, d) PAni-DBSA. Increase of 5,000 X.

CONCLUSION

Getting to know the influence of pilot scale and reaction time on structural and morphological characteristics of PAni-B

and PAni-DBSA can lead to important changes on structural properties related to electric characteristics.

In this study, polyaniline obtained in base and doped form was characterized as to identify significant changes in structure and morphology because synthesis has been carried out in a pilot scale and different reaction times.

Comparing both PAni forms, it is possible to identify the doping structure for PAni-DBSA by Raman spectroscopy due to the increase of the 890 and 1,343 cm^{-1} bands, assigned to polaronic structures, and the decrease of the 1,502 cm^{-1} band, indicating break of C=N bond.

The thermal behavior of PAni-B and PAni-DBSA shows that it is possible to distinguish components of the obtained polymers. However, some changes in temperature indicate that the combination of PAni and DBSA can change degradation temperature, increasing the onset temperature of DBSA degradation and reducing the onset temperature of PAni degradation. These changes affect weight losses percentage too, increasing weight losses percentage of PAni-DBSA.

Since changes in Raman spectra and TGA results of PAni-B and PAni-DBSA due to reaction time were not found, this variation seems to have little influence on polymer structure after doping.

The electrical conductivity is higher when the synthesis gets more time, indicating that reaction time can give some positive influence on conductivity.

The XRD result shows differences in crystalline peaks of PAni-B and PAni-DBSA that can be attributed mainly to the redoping process.

When the morphology shows the presence of fibers in the polymeric structure (reaction time of 50 and 170 min), the crystallinity index of PAni-B increases, which might indicate a correlation between these factors.

Whereas the formation of crystals on a pilot scale may change because of effects caused by water flow, the speed of polymerization can affect the formation of crystals too, causing random effects in different syntheses results and changing crystallinity index and morphology of PAni-B. However, these effects do not seem to be completely transferred to the doped form, probably due to many washing processes and association of PAni with a bulky molecule such as DBSA.

Evaluating the set of techniques, it is possible to assert that very important changes occur from PAni-B to PAni-DBSA. These changes allow getting a conductive behavior, as observed by Raman peaks and DIS. However, sensitivity *versus* reaction time is explained in detail by the last technique, in which it was possible to verify changes on 3 magnitude orders. It can be noticed that, for a pilot reactor system, it is required a time of 50 min for APS addition and 2 h more to process reaction mixing so that more conductive PAni is obtained.

ACKNOWLEDGEMENTS

Thanks to the Instituto de Aeronáutica e Espaço of the Departamento de Ciência e Tecnologia Aeroespacial (DCTA/IAE) that, through the Physical Chemistry Characterization Laboratory, Materials Division (AMR), provided the necessary structure and materials for this study.

AUTHOR'S CONTRIBUTION

Mazzeu MAC and Gonçalves ES conceived the idea and co-wrote the main text; Baldan MR and Gama AM discussed the results; Faria LK and Cardoso AM performed the experiments. All authors discussed the results and commented on the manuscript.

REFERENCES

Abdolahi A, Hamzah E, Ibrahim Z, Hashim S (2012) Synthesis of uniform polyaniline nanofibers through interfacial polymerization. Materials 5(8):1487-1494. doi: 10.3390/ma5081487

Abed MY, Youssif MA, Aziz HA, Shenashen MA (2014) Synthesis and enhancing electrical properties of PAni and PPA composites. Egyptian Journal of Petroleum 23(3):271-277. doi: 10.1016/j.ejpe.2014.08.003

Araujo JR, Adamo CB, Robertis E, Kuznetsov AY, Archanjo BS, Fragneaud B, Achete CA, De Paoli MA (2013) Crystallinity, oxidation states and morphology of polyaniline coated curauá fibers in polyamide-6 composites. Compos Sci Tech 88:106-112. doi: 101016/jcomposcitech.2013.08.039

Ashraf A (2014) Electrical conductivity measurement of polyaniline and its composites; [accessed 2016 Jun 14]. https://www.Researchgate.net/publication/271840942_Electrical_Conductivity_measurement_of_polyaniline_and_its_composites

Babazadeh M (2009) Aqueous dispersions of DBSA-doped polyaniline:

one-pot preparation, characterization and properties study. J Appl Polymer Sci 113(6):3980-3984. doi: 10.1002/app.30460

Barsoukov E, MacDonald JR (2005) Impedance spectroscopy theory, experiment, and applications. 2nd Edition. New Jersey: John Wiley & Sons.

Belaabed B, Lamouri S, Naar N, Bourson P, Hamady SOS (2010) Polyaniline-doped benzene sulfonic acid/epoxy resin composites: structural, morphological, thermal and dielectric behaviors. Polymer J 42:546-554. doi: 10.1038/pj.2010.41

Bhadra S, Khastgir D (2008) Determination of crystal structure of polyaniline and substituted polyanilines through powder X-ray diffraction analysis. Polymer Test 27(7):851-857. doi: 101016/j.polymertesting.2008.07.002

Bierwagen G (2001) Next generation of aircraft coatings systems. J Coating Tech 73(915):45-52. doi: 10.1007/BF02730030

Cirić-Marjanović G, Trchová M, Stejskal J (2008) The chemical oxidative polymerization of aniline in water: Raman spectroscopy. J Raman Spectros 39(10):1375-1387. doi: 10.1002/jrs.2007

Engert C, Umapathy S, Kiefer W, Hamaguchi H (1994) Dynamic structure of charge carrier in polyaniline by near-infrared excited resonance Raman spectroscopy. Chem Phys Lett 218(1-2):87-92. doi: 10.1016/0009-2614(93)E1468-V

Faez R, Rezende MC, Martin IM, Paoli MA (2000) Polímeros condutores intrínsecos e seu potencial em blindagem de radiações eletromagnéticas. Polímeros 19(3):130-137. doi: 10.1590/S0104-14282000000300009

Franchitto M, Orlando AJF, Faez R, Rezende MC, Martin IM (2007) Measurements of reactivity and complex permittivities of radar absorbing materials based on conducting polymers. Proceedings of the 2007 Progress in Electromagnetics Research Symposium; Beijing, China.

Fratoddi I, Venditti I, Cametti C, Russo MV (2015) Chemiresistive polyaniline-based gas sensors: a mini review. Sensor Actuator B Chem 220:534-548. doi: 10.1016/j.snb.2015.05.107

Galiani PD, Malmonge JA, Santos DP, Malmonge LF (2007) Compósitos de borracha natural com polianilina. Polímeros 7(2):93-97. doi: 10.1590/S0104-14282007000200007

Gul S, Shahb AA, Bilal S (2013) Synthesis and characterization of processable polyaniline salts. J Phys Conf 439(2013):012002. doi: 10.1088/1742-6596/439/1/012002

Huang J, Kaner RB (2006) The intrinsic nanofibrillar morphology of polyaniline. Chem Commun (Camb) (4):367-376. doi: 10.1039/B510956f

Ibrahim KA (2013) Synthesis and characterization of polyaniline and poly(aniline-co-o-nitroaniline) using vibrational spectroscopy. Arabian Journal of Chemistry. doi: 10.1016/j.arabjc.2013.10.010. In press.

Jaymand M (2013) Recent progress in chemical modification of polyaniline. Prog Polymer Sci 38(9):1287-1306. doi: 10.1016/j.progpolymsci.2013.05.015

Joo J, Lee CY (2000) High frequency electromagnetic interference shielding response of mixtures and multilayer films based on conducting polymers. J Appl Phys 88(1):513-518. doi: 10.1063/1.373688

Kohut-Svelko N, Reynaud S, François J (2005) Synthesis and characterization of polyaniline prepared in the presence of nonionic surfactants in an aqueous dispersion. Synthetic Met 150(2):107-114. doi: 10.1016/j.synthmet.2004.12.022

Krukiewicz K, Katunin A (2016) The effect of reaction medium on the conductivity and morphology of polyaniline doped with camphorsulfonic acid. Synthetic Met 214:45-49. doi: 10.1016/j.synthmet.2016.01.017

Kumar SA, Bhandari H, Sharma C, Khatoon F, Dhawan SK (2013) A new smart coating of polyaniline-Si02 composite for protection of mild steel against corrosion in strong acidic medium. Polymer Int 62(8):1192-1201. doi: 10.1002/pi.4406

Laska J, Widlarz J (2005) Spectroscopic and structural characterization of low molecular weight fractions of polyaniline. Polymer 46(5):1485-1495. doi: 10.1016/j.polymer.2004.12.008

Luo C, Peng H, Zhang L, Lu G-L, Wang Y, Travas-Sejdic J (2011) Formation of nano-microstructures of polyaniline and its derivatives. Macromolecules 44(17):6899-6907. doi: 10.1021/ma201350m

MacDiarmid AG (2001) "Synthetic Metals": a novel role for organic polymers (Nobel Lecture). Angew Chem Int Ed 40(14):2581-2590. doi: 10.1002/1521-3773(20010716)40:14<2581::AID-ANIE2581>3.0.CO;2-2

Manjunath BR, Venkataraman A, Stephen T (1973) The effect of moisture present in polymers on their X-ray diffraction patterns. J Appl Polymer Sci 17(4):1091-1099. doi: 10.1002/app.1973.070170407

Mažeikienė R, Tomkutė V, Kuodis Z, Niaura G, Malinauskas A (2007) Raman spectroelectrochemical study of polyaniline and sulfonated polyaniline in solutions of different pH. Vib Spectros 44(2):201-208. doi: 101016/j.vibspec.2006.09.005

Moravková Z, Trchová M, Exnerová M, Stejskal J (2012) The carbonization of thin polyaniline films. Thin Solid Films 520(19):6088-6094. doi: 101016/j.tsf.2012.05.067

Nithyaprakash D, Chandrasekaran J, Punithaveni B, Sasikumar L (2014) The study of optical, dielectric and optoelectronic properties of dodecylbenzene sulfonic acid doped polyaniline. Optik 125:5343-5347. doi: 101016/j.ijleo.2014.06.057

Nobrega MM, Silva HB, Constantino VRL, Temperini MLA (2012) Spectroscopic study on the structural differences of thermally induced cross-linking segments in emeraldine salt and base forms of polyaniline. J Phys Chem B 116(48):14191-14200. doi: 101021/jp309484e

Panah NB, Payehghadr M, Danaee I, Nourkojouri H, Sharbatdaran M (2012) Investigation of corrosion performance of epoxy coating containing polyaniline nanoparticles. Iran Polym J 21(11):747-754. doi: 10.1007/s13726-012-0080-8

Pouget JP, Józefowicz ME, Epstein AJ, Tang X, MacDiarmid AG (1991) X-ray structure of polyaniline. Macromolecules 24(3):779-789. doi: 101021/ma003a022

Rinaldi G, Huber T, McIntosh H, Lebrun L (2012) Corrosion sensor development for condition-based maintenance of aircraft. International Journal of Aerospace Engineering (2012):Article ID 684024, 11 pages. doi: 10.1155/2012/684024

Roichman Y, Titelman GI, Silverstein MS, SiegmannA, Narkis M (1999) Polyaniline synthesis: influence of powder morphology on conductivity of solution cast blends with polystyrene. Synthetic Met 98(3):201-209. doi: 10.1016/S0379-6779(98)00190-8

Sathiyanarayanan S, Azim SS, Venkatachari G (2008). Corrosion

protection of magnesium alloy ZM21by polyaniline-blended coatings. J Coat Technol Res 5(4):471-477. doi: 10.1007/s11998-008-9097-5

Saravanan S, Mathai CJ, Anantharaman MR, Venkatachalam S, Prabhakaran PV (2006) Investigation on the electrical and structural properties of polyaniline doped with camphor sulphonic acid. J Phys Chem Solid 67(7):1496-1501. doi: 101016/j-jpcs.2006.01.100

Shakoor A, Rizvi TZ (2010) Raman spectroscopy of conducting poly (methylmethacrylate)/polyanilinedodecylbenzenesulfonate blends. J Raman Spectros 41(2):237-240. doi: 10.1002/jrs.2414

Stejskal J, Sapurina I, Trchov M (2010) Polyaniline nanostructures and the role of aniline oligomers in their formation. Progr Polymer Sci 35(12):1420-1481. doi: 10.1016/j.progpolymsci.2010.07.006

Soares B, Leyva ME, Barra GMO, Khastgir D (2006) Dielectric behavior of polyaniline synthesized by different techniques. Eur Polymer J 42(3):676-686. doi: 101016/eurpolymj.2005.08.013

Vivekanandan J, Ponnusamy V, Mahudeswaran A, Vijayanand PS (2011) Synthesis, characterization and conductivity study of polyaniline prepared by chemical oxidative and electrochemical methods. Arch Appl Sci Res 3(6):147-153.

Zeng X-R, Ko T-M (1998) Structure and properties of chemically reduced polyanilines. Polymer 39(5):1187-1195. doi: 10.1016/S0032-3861(97)00381-9

Zilberman M, Titelman GI, Siegmann A, Haba Y, Narkis M, Alperstein D (1997) Conductive blends of thermally dodecylbenzene sulfonic acid-doped polyaniline with thermoplastic polymers. J Appl Polymer Sci 66(2):243-253. doi: 10.1002/(SICI)1097-4628(19971010)66:2<243::AID-APP5>3.0.CO;2-W